

Research Article

Hybrid Integration of Transforms with Neural Network based Fusion Techniques for clinical and Healthcare Applications

B.Rajalingam¹, R.Santhoshkumar², Dr. G.Govinda Rajulu³, P.Deepan⁴, S. Bavankumar⁵, Dr. P. Santosh Kumar Patra⁶

ABSTRACT

The prime objective of Hybrid Multimodal Medical Image Fusion (HMMIF) method is preservation of important features of images and details about various images from source for creating a visually robust enough single fused image provides a very promising diagnostic tool with numerous clinical and healthcare applications. The Non subsampled shearlet Transform (NSST) with Pulse Coupled Neural Network (PCNN) based hybrid algorithms are proposed for MMIF in this paper. In the proposed method, initially input images are decomposed to less and high frequencies with the application of NSST. The components with lesser frequency are applied with averaging fusion rule. The maximum fusion rule with PCNN is applied on high frequency components. The coefficients produced by every frequency bands are inverse transformed to provide fused images. The proposed algorithms provide the best fused images without distortion and false artefacts. Comparison of proposed technique is done with the pre-existing conventional techniques. The images obtained by fusing both sources' content with the help of the above algorithm gives the best with respect to visualization and diagnosis of the condition.

Key words: Multimodal Medical Image Fusion (MMIF), Computed Tomography, Magnetic Resonance Imaging, Positron emission Tomography, Single Photon Emission Tomography and Healthcare applications.

1 INTRODUCTION

Various medical images for clinical diagnosis are provided by the development of medical imaging and information processing technologies. These are widely applied in diagnosing diseases, surgery, and radiotherapy. Every sensor got from various imaging modalities have different benefits and gives different information about the human body. Hence a complete diagnosis cannot be obtained from a single image and doctors need combination of various imaging modalities to get a more detailed data about the tissue or organ. A single medical picture modality is incapable of providing comprehensive and precise information. As a result, not every modality may display all of the relevant information about a specific condition. As a result, physicians always advise patients to undergo a variety of imaging modalities before making a definitive diagnosis. Almost majority health centres lack the ability to obtain combined details about multiple modalities using a single system. Because of the exorbitant

^{1,2,3}Associate Professor, ⁵Assistant Professor, ⁶Principal & Professor

^{1,2,3,4,5,6}Department of CSE, St. Martin's Engineering College, Secunderabad, Telangana, India

¹rajalingam35@gmail.com, ²santhoshkumar.aucse@gmail.com, ³rajulug7@gmail.com, ⁴deepanp87@gmail.com

⁵sbavankumar55@gmail.com

expense of the technology, no hospital in India has hybrid modality imaging. Even if scanners become accessible, the cost of imaging will be too expensive for people.

In the near future, such a facility may not be offered to patients from economically developing countries like India. A PET-CT scanner is a popular hybrid modality machine that works on the premise of overlaying both modality images. The new PET-MRI scanner is still in the works. As a result, there is a social and pressing demand for a software solution that can aggregate information from many imaging modalities in a single frame at a low cost. Multimodality medical image fusion is one such software solution (MMIF). It is the process of combining all important and complimentary information from two or more modality images to create a new enriched single frame. It should also assist radiologists in obtaining all anatomical structures from all modalities and improving visibility of anomalies.

This research work focuses on the NSST as a decomposition tool. In this algorithm, the flexible multiresolution, shift-invariant and lossless feature of the NSST is linked to global coupling as well as pulse synchronization characteristic of Pulse Coupled Neural Network. The Pulse Coupled Neural Network is similar to the functioning of human visual neural system. The PCNN produces a series of binary pulse images when stimulated with a grayscale or color image. PCNN is different from ANN in the sense that it does not train like ANN. The common additive coupling is used in ANN, whereas the PCNN uses modulatory coupling. The additive nature of the neighboring neurons helps in activation with no input in ANN. On the contrary in PCNN, the neuron doesn't get activated by the coupling input. This serves to be a vital and beneficial part in the image processing. The PCNN is used as a nonlinear filter to select the coefficients in the NSST decomposed images. The combining method is applied separately for the regions of less frequency and the regions of higher frequency and at last the inverse NSST is utilized to get images that are fused. The future work can be extended using covid 19 affected input medical images.

Here a new PCNN dependent hybrid image fusion method is introduced and discussed. Section 1 describes the introduction of MMIF. Section 2 describes the presented hybrid fusion algorithm. Section 3 compares the capability of the existing and proposed fusion technique. Section 4 concludes the paper.

2 LITERATURE REVIEW

Lei Wang, *et al.* [1] proposed a new dependency model, known as explicit generalized gaussian density dependency model created by the shift-invariant shearlet transform to solve these problems. Lei Wang, *et al.* [2] proposed a fusion technique in three dimensional shearlet space to make it right the drawback. While the commonly utilized average-maximum fusion rule cannot get any global data but only the local data. It is used in a local window region. Jingming Yang, *et al.* [3] developed a new Computed Tomography and Magnetic Resonance Imaging image fusion algorithm from a NSST and Compressive Sensing (CS) theory. Studies concluded that this enhances the information of the fused images along with reducing the complexity in calculating. Niu Ling, and colleagues [4] demonstrated a new method for fusion of medical images using shearlet transform and CS model. In comparison using simulation experiment this method is better than the current methods such as non-negative matrix factorization. K.N. Narasimha Murthy, *et al.* [5] proposed a novel technique in which shearlet transform is employed on image with the Singular Value Decomposition to enhance the details of the clinical photographs. Here 2 various PET and MRI are fused. Xingbin Liu, *et al.* [6] proposed a new MMIF algorithm from a moving frame-based decomposition framework and NSST.

Study results confirm that this technique has enhanced capability in comparison with traditional techniques with respect to visual effects and objective criteria. Weiguo Wan, and colleagues [7] demonstrated a novel remote sensing image fusion scheme in NSST domain. An enhancement strategy is modelled to resolve the deficiency of spatial information in Multiresolution Analysis (MRA)-dependent techniques succeeding to the intensity–hue–saturation color space transform. Weiwei Kong, *et al.* [8] proposed a new fusion method for multimodal sensor medical images, using local difference in non-subsampled domain. The demonstrated fusion technique was employed in various experiments and the results demonstrate it as a straightforward and effective technique in comparison with the standard techniques, with respect to the visual assessment by subjects and the result objective evaluation. The author and colleagues [9] demonstrated a novel MMIF technique in NSST domain. Here multiscale and multidirectional representations of the source images are obtained by the Non Subsampled Shearlet Transformation decomposition.

Lu Tang, *et al.* [10] demonstrated a novel MMIF technique using discrete Tchebichef moments as well as pulse coupled neural network. The study results demonstrate this scheme is has improved performance in comparison to the pre-existing techniques and it has enhanced efficiency in processing medical images of varying modalities. Xin Jin, *et al.* [11] proposed a novel method to fuse Computed Tomography, Magnetic Resonance Imaging as well as PET images into a single image. A new 2-stage scheme for fusing medical images with a Non-Subsampled Shearlet Transformation and simplified PCNN, is used in the Hue-Saturation-Value (HSV) color space. Jingming Xia, and colleagues [12] used a medical image fusion algorithm along with sparse representation and PCNN. The final result after the study demonstrate that the algorithm of gray and color image fusion is higher than the contrast algorithm. Weiwei Kong, and colleagues. [13] demonstrated a new technique for fusing images with NSST and improved PCNN. Being an effective multi-resolution analysis tool, Non Subsampled Shearlet Transformation is utilized for obtaining a series of sub bands which has varying scales and directions. The author and his colleagues [14] demonstrated a new fusion scheme for multimodal medical images using the features of the multi-scale transformation and deep convolutional neural network. The author and his colleagues [15] proposed a new fusion scheme for NSST using simplified model of PCNN model. This technique is visually compared with 5 best pre-existing schemes, with respect to 5 fusion performance parameters.

3 Proposed Hybrid Fusion Algorithm (NSST-PCNN)

Here, NSST and PCNN techniques are employed for input multimodal medical images. Figure 1 shows the block diagram of hybrid algorithm (NSST-PCNN).

Hybrid Integration of Transforms with Neural Network based Fusion Techniques for clinical and Healthcare Applications

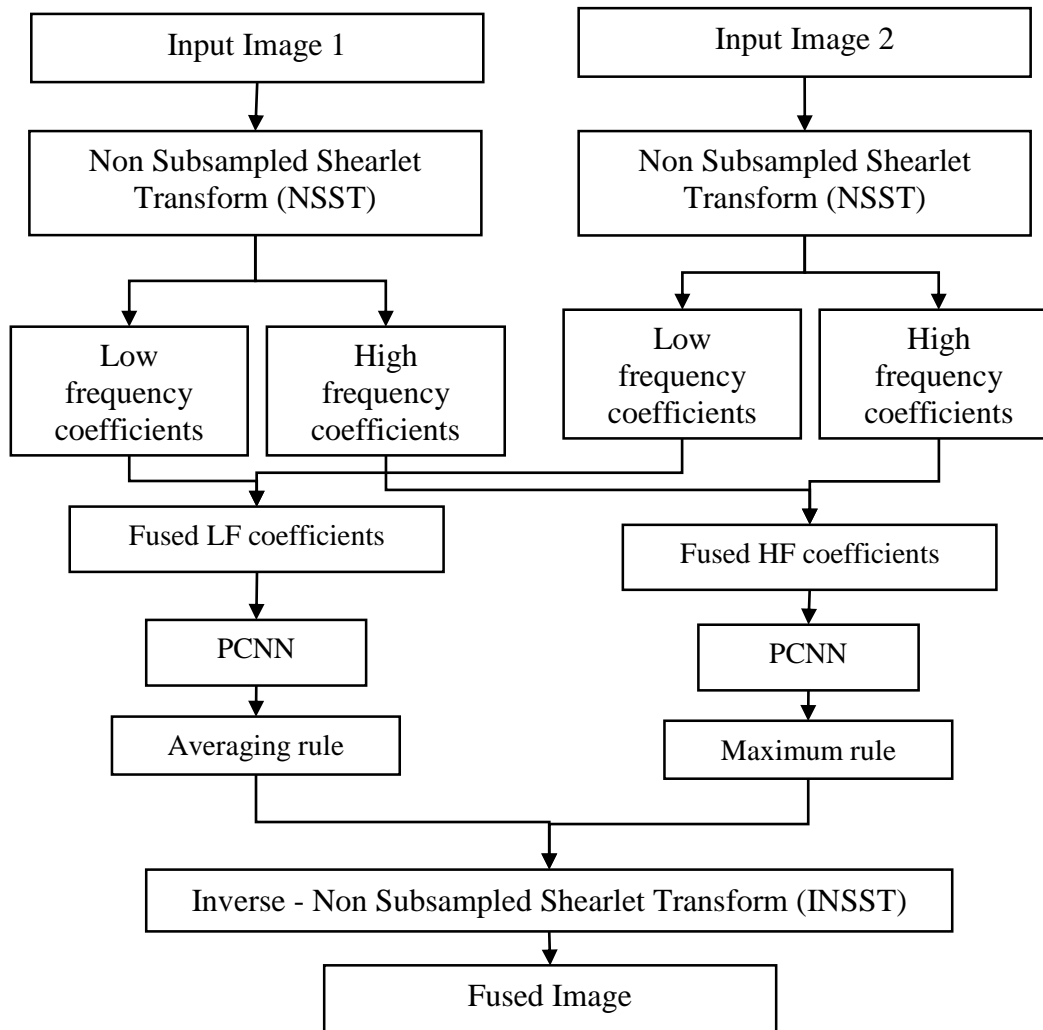


Fig. 1 Block diagram for proposed hybrid algorithm (NSST- PCNN)

3.1 Procedural steps for proposed hybrid algorithm (NSST–PCNN)

Step 1: The perfectly registered input images of the same person and same spatial part are converted into multiresolution image using NSST.

Step 2: Apply PCNN to low and high frequency regions of both the images and obtain the firing map.

Step 3: Fuse the low pass coefficients using averaging fusion rule.

Step 4: Fuse the high pass coefficients using the maximum fusion rule.

Step 5: Apply inverse NSST to the get fused image

Step 6: Analyze the fused image both subjectively and objectively

Fusion Rule of Low Frequency Region

The low pass coefficients of the image A is denoted as LL_A and that of the image B as LL_B . The firing map obtained by applying PCNN to the low pass coefficients of the image A is

denoted as M1 and that of the image B is denoted as M2. Fusion of these coefficients are done by averaging fusion rule. Below equation (2) represents the averaging fusion rule,

$$F_L = \begin{cases} LL_A & M_1 \geq M_2 \\ LL_B & otherwise \end{cases} \quad (1)$$

$$C_F = \frac{1}{2}(C_i^1 + C_i^2) \quad (2)$$

where, C_F is the combined coefficient, C_i^1, C_i^2 are the coefficients of the input images X and Y.

Fusion Rule of High Frequency Region

The maximum coefficient fusion rule is selected to take the fusion into area of increased frequency. In image A, the high frequency coefficient's characteristic variable C is depicted in Equation (3),

$$C_j^\varepsilon(A, k) = \max_{p \in Q} (D_j^\varepsilon(A, p)) \quad (3)$$

where, j - represents the shearlet coefficient,

ε - is the decomposition levels and takes the value 1, 2, 3 and k is the spatial position of the shearlet coefficient.

Q - is a small area by the centre of k,

D - depicts the detail coefficient of the shearlet transform,

p - is the pixel which lies in the area Q.

similarly, the characteristic variable for the image B is briefed. The shearlet coefficient with the maximal characteristic variable is chosen.

$$Z_j^\varepsilon(A, k) = \begin{cases} 1, & C_j^\varepsilon(A, k) > C_j^\varepsilon(B, k) \\ 0, & C_j^\varepsilon(A, k) \leq C_j^\varepsilon(B, k) \end{cases} \quad (4)$$

$$Z_j^\varepsilon(B, k) = \begin{cases} 1, & C_j^\varepsilon(B, k) > C_j^\varepsilon(A, k) \\ 0, & C_j^\varepsilon(B, k) \leq C_j^\varepsilon(A, k) \end{cases} \quad (5)$$

The equations (4) and (5) are changes as per majority representation method.

$$Z_j^\varepsilon(A, k) = \begin{cases} 1, & \sum_{k \in Q} Z_j^\varepsilon(A, k) \geq 5 \\ 0, & \sum_{k \in Q} Z_j^\varepsilon(B, k) < 5 \end{cases} \quad (6)$$

$$Z_j^\varepsilon(B, k) = \begin{cases} 1, & \sum_{k \in Q} Z_j^\varepsilon(A, k) = 0 \\ 0, & \sum_{k \in Q} Z_j^\varepsilon(A, k) = 1 \end{cases} \quad (7)$$

Hybrid Integration of Transforms with Neural Network based Fusion Techniques for clinical and Healthcare Applications

The fusion rule for the high-frequency is obtained by referring to equations (6) and (7) as,

$$D_j^e(f, k) = Z_j^e(A, k).D_j^e(A, k) + Z_j^e(B, k).D_j^e(B, k) \quad (8)$$

All the vertical, horizontal and diagonal high frequencies of the images undergo fusion. $D_j^e(f, k)$ - represents the high frequency subband images.

3.2 Non Subsampled Shearlet Transform (NSST)

Shearlet transform has a robust mathematical structure and is a potential tool for Multiscale Geometric Analysis (MGA). It is localized and decays fast in spatial domain. Shearlets satisfy parabolic scaling law. It has a good sensitivity to direction. The number of directions is doubled in every next finer scale. Still, pseudo Gibbs phenomenon and other inefficiencies occur in the fusion results as it not shift invariant. [16] Hence to eliminate this shortcoming invariant version of shearlet transform known as NSST is created.

3.3 Pulse Coupled Neural Network (PCNN)

A single layer two-dimensional array of laterally linked pulse-coupled neurons undergo image fusion by PCNN. A direct communication takes place among the image pixels as well as network neurons and the gray value of each pixel often is related to the external stimulus of every neuron. The PCNN model is shown in Figure 2. It has receptive field, the modulation field, and the pulse generator. The receptive field bifurcates into 2 fields. They are linking and feeding fields. The input signal is received by a neuron from others as well as external sources from channels F as well as L . F Channel is the feeding input, F_{ij} that obtains the input from the external sources and the output of other neurons. L channel is the linking input L_{ij} where the inputs are received from the neighboring neurons in the linking range, typically within 3×3 or 5×5 . So a neuron is interlinked to the nearby neurons to create a global coupling network. The linking strength β decides the strength of the coupling relation within the group of neuron. [17], [18]

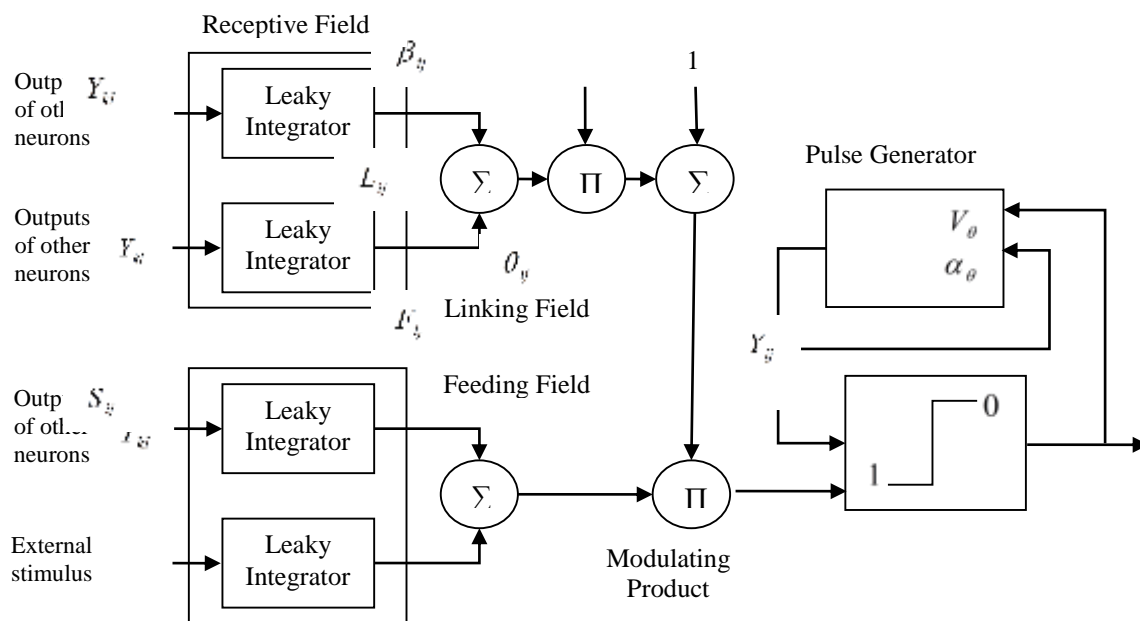


Fig. 2 Basic model of PCNN neuron

where,

Y_{kl} - Neighboring neurons output	Y_{ij} - Output
S_{ij} - External Stimulus	V_{θ} - Magnitude scaling term
F_{ij} - Feeding Input	α_{θ} - Decay constant of threshold potential
θ_{ij} - Threshold Value	β_{ij} - Linking strength of the neuron
U_{ij} - Internal Activity	L_{ij} - Linking Input

The internal activity U_{ij} is activated by modulation of feeding field with linking field. The pulse generator produces a threshold value θ_{ij} . The internal activity compares the threshold value θ_{ij} depending on the step response. If $U_{ij} > \theta_{ij}$, the output is '1'; otherwise the output is '0'. Initially a neuron gets fired, it starts to correspond with its neighbors and makes closest neighbors to fire such that it is given support using interconnections. As the internal activity $U_{ij} >$ dynamic threshold θ_{ij} , The neurons that corresponds to it fires giving the output $Y_{ij} = 1$.

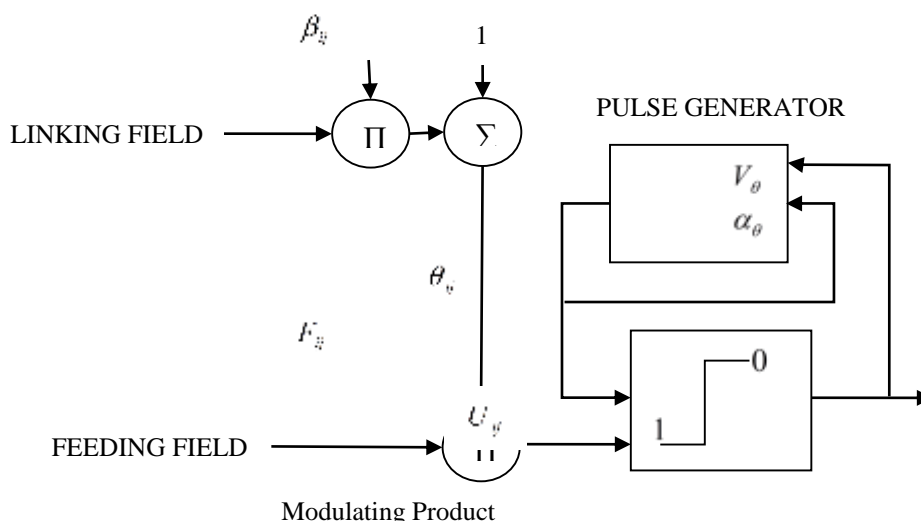


Fig. 3 Simplified model of PCNN neuron

Simultaneously, There is an immediate raise in the θ_{ij} of the fired neuron for preventing it from getting fired once more, and the neurons' output $Y_{ij} = 0$. If θ_{ij} of a neuron decreased as less than or equal to its U_{ij} once more, the neuron will also fire again to cause impulse sequence. U depicts the internal activity that has F and L which are the feeding input and the linking input respectively. Therefore, the state of a neighborhood affects the state of neuron. So, activation of a neuron, could activate the pixels having similar gray values around it in the next iteration. The simplified model of Pulse Coupled Neural Network neuron is shown in Figure 3.

Mathematical Equations of PCNN Neuron

The discrete mathematical equations of each neuron of conventional PCNN can be described as follows.

1. Feeding field

The neurons' traditional PCNN feeding field is dependent on the output in the preceding iteration step $F_{ij}(n-1)$, S_{ij} and Y_{kl} depicts the external stimulus and weighted output of the nearby neurons respectively. The feeding field is represented as

Hybrid Integration of Transforms with Neural Network based Fusion Techniques for clinical and Healthcare Applications

$$F_{ij}(n) = e^{-\alpha_L} F_{ij}(n-1) + S_{ij} + V_F \sum_{kl} M_{ij,kl} Y_{kl}(n-1) \quad (9)$$

where, α_L is decay constant, S_{ij} is the external stimulus, V_F depicts magnitude of scaling term, $M_{ij,kl}$ depicts the output of other neighboring neurons' synaptic weight strength. The pixel values of the static image There are fixed pixel values for static images in the image processing applications. So the equation (10) can be simplified as

$$F_{ij}(n) = S_{ij} \quad (10)$$

2. Linking field

The traditional Pulse Coupled Neural Network linking field of the neuron is based on the value of the preceding one $L_{ij}(n-1)$, $Y_{kl}(n-1)$ depicts the weighted output of other neighboring neurons as

$$L_{ij}(n) = e^{-\alpha_L} L_{ij}(n-1) + V_L \sum_{kl} W_{ij,kl} Y_{kl}(n-1) \quad (11)$$

here, α_L - decay constant of the linking field, V_L - magnitude scaling term,

$W_{ij,kl}$ are the synaptic gain strength. In the case of static input images, the above equation can be simplified as

$$L_{ij}(n) = V_L \sum_{kl} W_{ij,kl} Y_{kl}(n-1) \quad (12)$$

3. Internal activity

The following formula is used to calculate the internal activity of traditional pulse couples neuronal network by changing the feeding field into linking field

$$U_{ij}(n) = F_{ij}(n)[1 + \beta L_{ij}(n)] \quad (13)$$

here, β - linking strength of the neuron

4. Threshold potential

The threshold potential is given by

$$\theta_{ij}(n) = e^{-\alpha_\theta} \theta_{ij}(n-1) + V_\theta Y_{ij}(n-1) \quad (14)$$

here, α_θ is decay constant of threshold potential, V_θ depicts magnitude scaling term

5. Output of neuron

The following defines the output of Pulse Controlled Neural Network

$$Y_{ij}(n) = \begin{cases} 1 & U_{ij}(n) \geq \theta_{ij}(n) \\ 0 & \text{otherwise} \end{cases} \quad (15)$$

4. EXPERIMENTAL RESULTS

The proposed HMMIF method is studied on pilot study sets combination of CT/MRI, MRI/PET finally MRI/SPECT of the brain neurocysticercosis affected patients, degenerative and neoplastic diseases. The combination of input images each pair of both CT and MRI slices, MRI/PET slices and Magnetic Resonance Imaging and SPECT slices of the same patient are choosing with the help of similarities in anatomy and function. The fusion results of this hybrid image fusion method and other existing techniques are shown in figures 4, 5, 6, 7, 8 and 9. Input images collected from online databases Harvard medical school[19] and radiopedia [20].

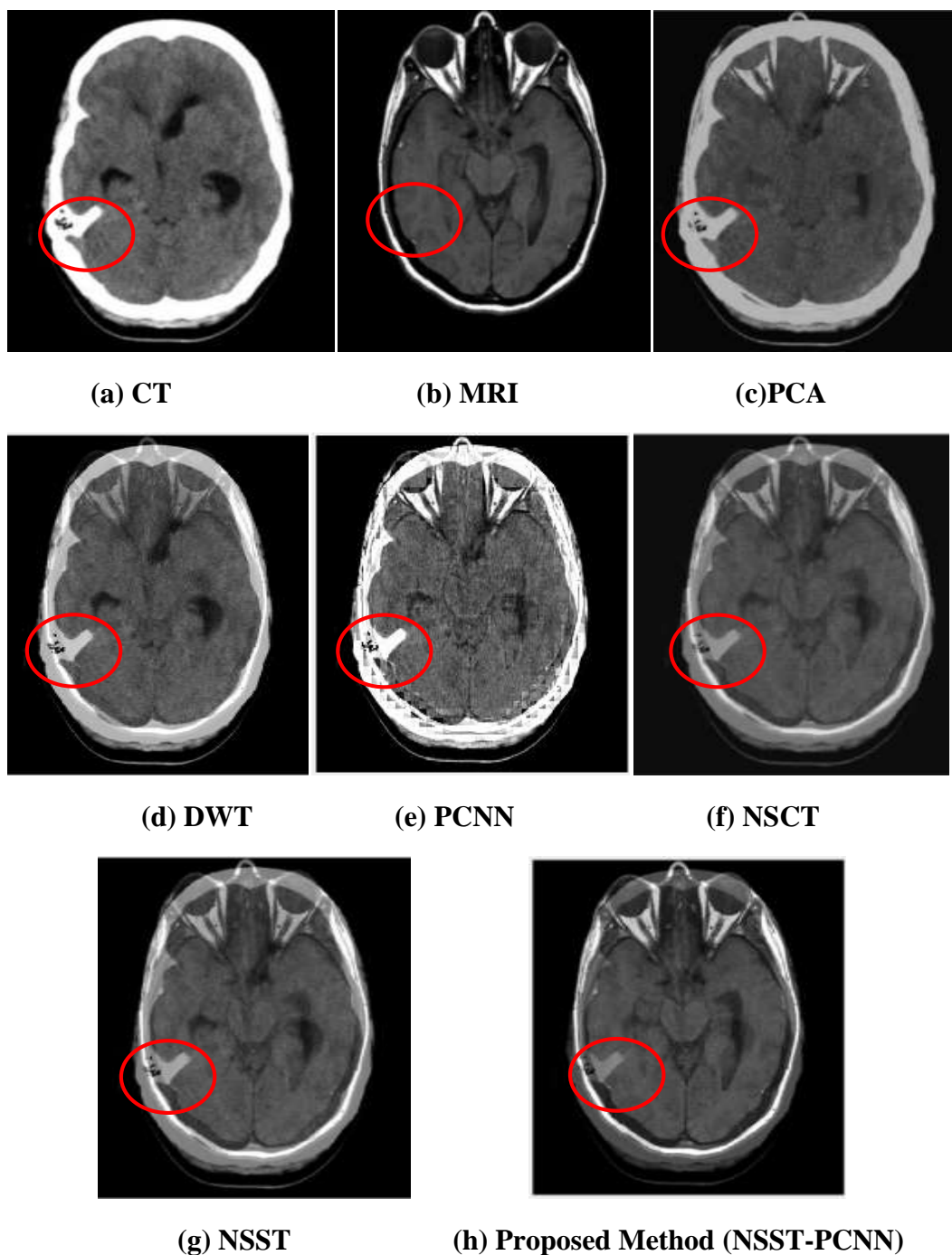


Fig. 4 Experimental results for neurocysticercosis disease affected images (Set 1)

Hybrid Integration of Transforms with Neural Network based Fusion Techniques for clinical and Healthcare Applications

Six different sets of CT/MRI, MRI/PET and MRI/SPECT images are taken for the image fusion. The first set of input images represents the neurocysticercosis disease affected images taken from CT and MRI scanners respectively. Second set of input images represents the metastatic bronchogenic carcinoma disease affected brain images in the combination of MRI/SPECT.

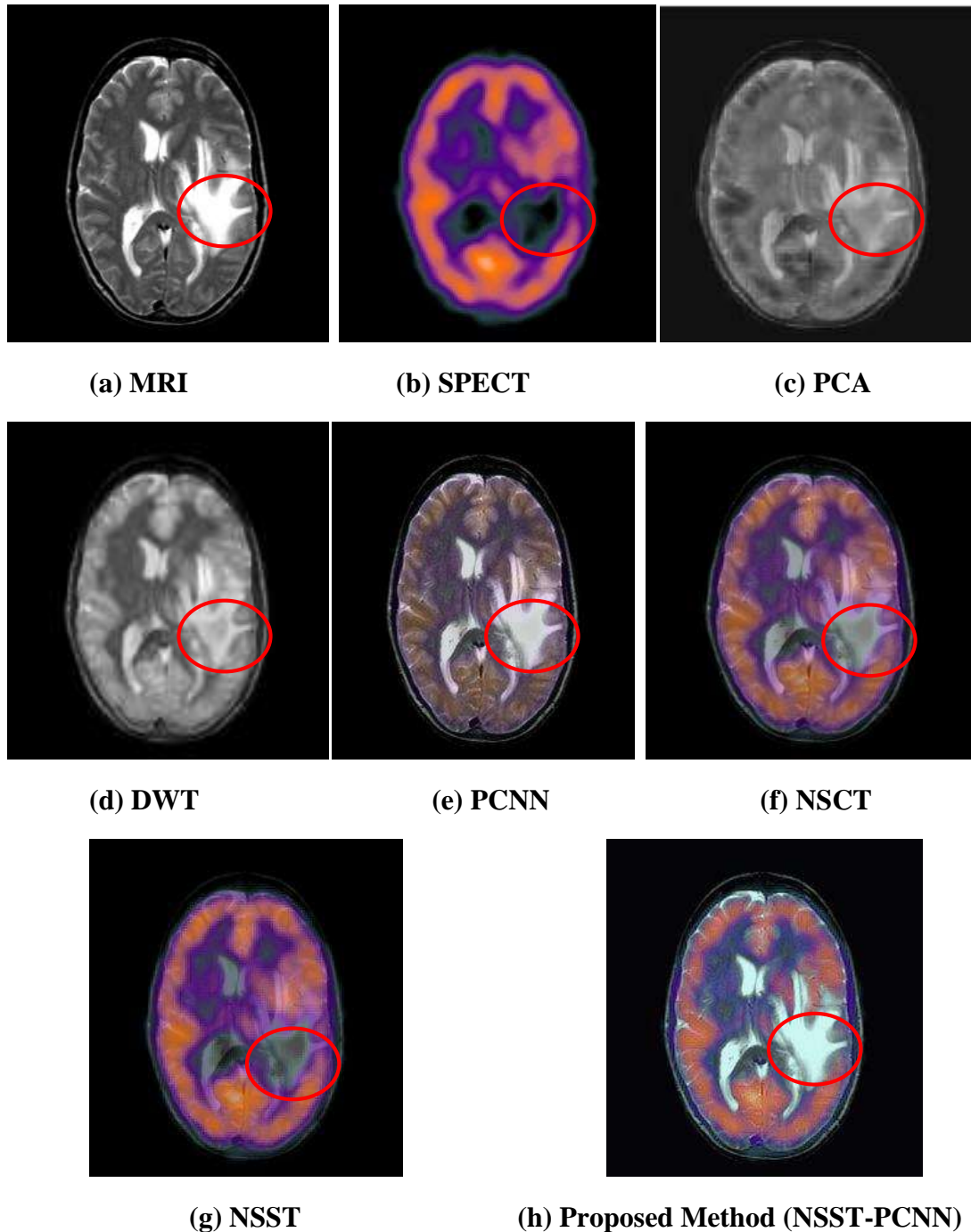


Fig.6 Experimental results of metastatic bronchogenic carcinoma affected images(Set 2)

Third and fourth sets of input images represent the astrocytoma and anaplastic astrocytoma disease affected brain images in the combination of MRI/SPECT respectively. Fifth and sixth sets of input images represent the alzheimer's and mild alzheimer's disease affected brain images in the combination of MRI/SPECT and MRI/PET respectively. The table shows the fusion

results of the same input images are using PCA, DWT, PCNN, NSCT, NSST and the proposed hybrid technique using the combination of NSST – PCNN.

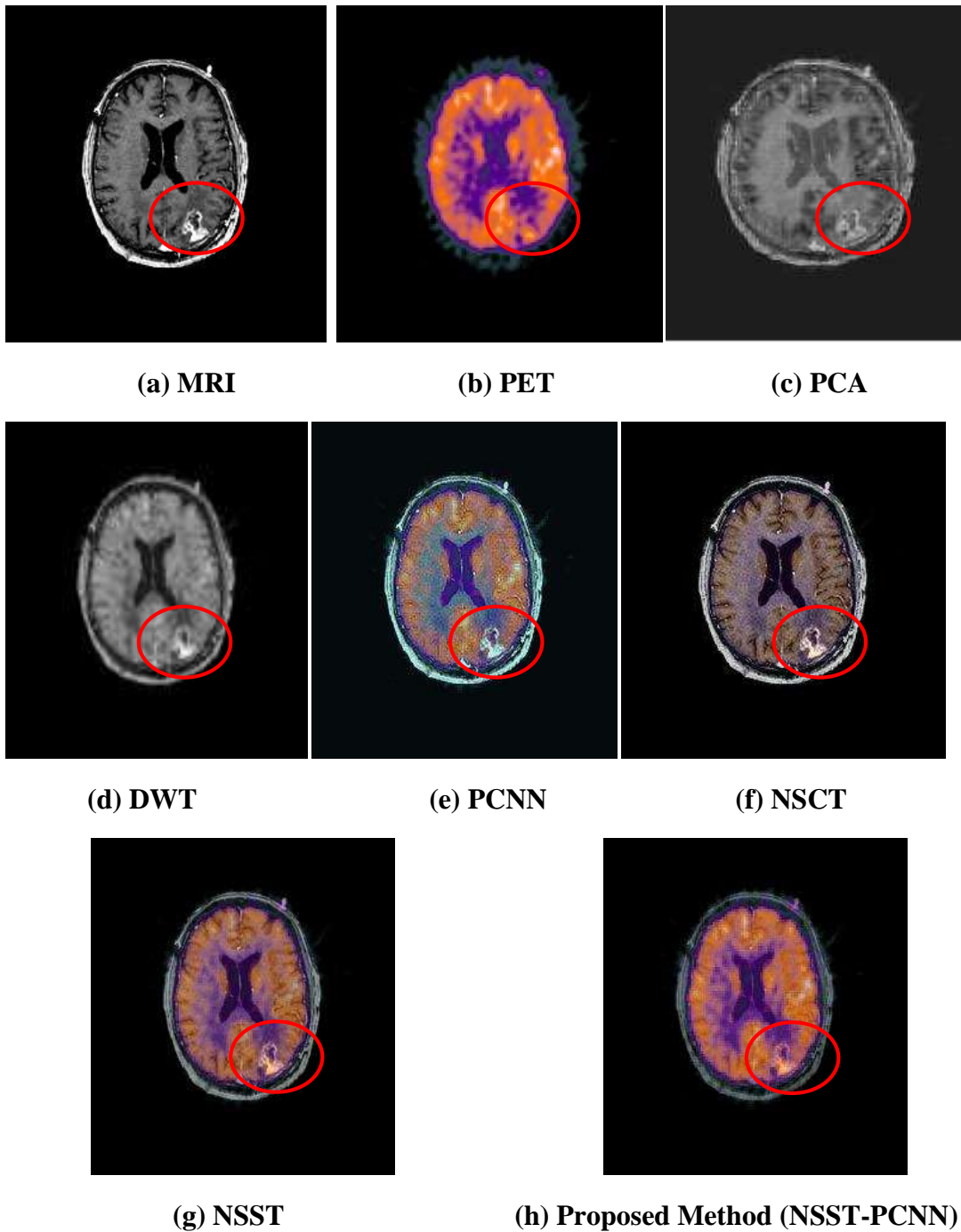


Fig. 7 Experimental results for astrocytoma disease affected images (Set 3)

Hybrid Integration of Transforms with Neural Network based Fusion Techniques for clinical and Healthcare Applications

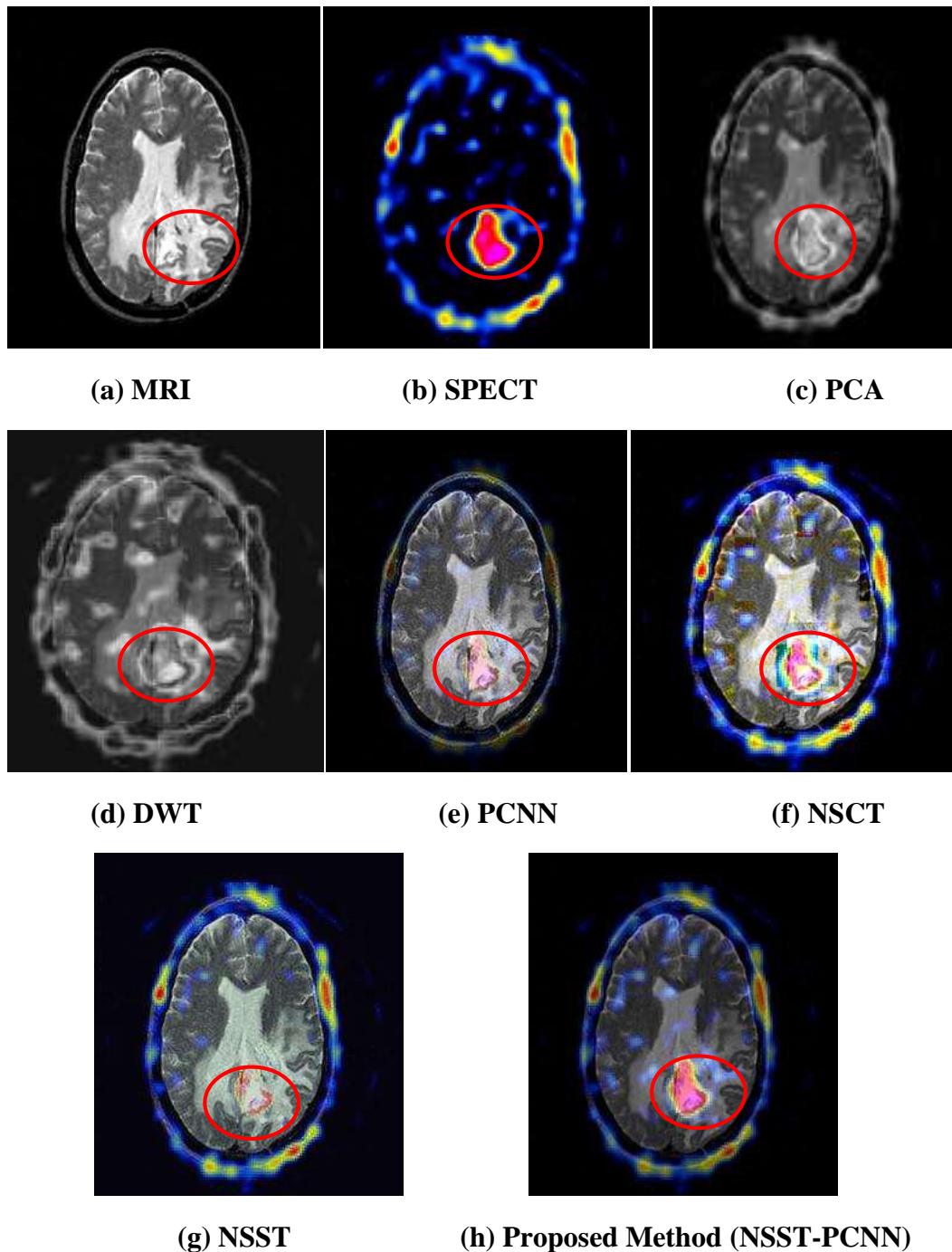
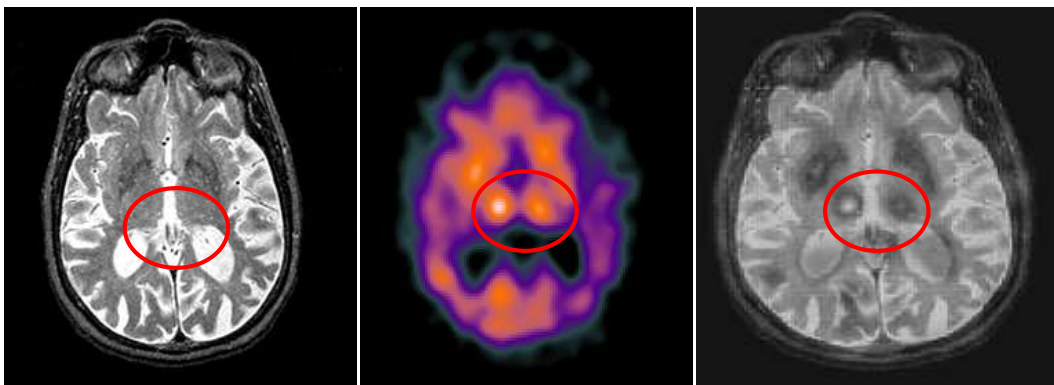


Fig. 8 Experimental results for anaplastic astrocytoma affected images (Set 4)

Out of all the traditional fusion techniques, the simulation result of the proposed hybrid technique provides better performances both qualitatively and quantitatively. Quantitative analysis is required for analyzing the image obtained by fusion. The effectiveness of the fused image is proved by evaluating the values of the performance metrics results as shown in Tables 1 and 2. One complete dataset of CT and MRI, MRI and PET and MRI and SPECT are fused. From the tabulated values, it is understood that the proposed NSST-PCNN method has better values for Fusion factor, IQI, EQM, mSSIM, STD, MI and PSNR than the existing conventional techniques.[19], [20]



(a) MRI

(b) SPECT

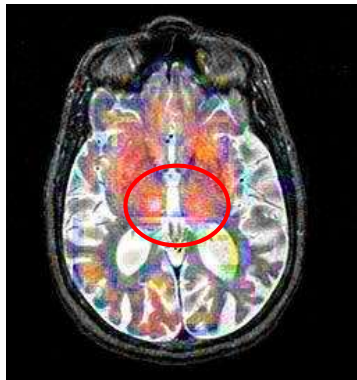
(c) PCA



(d) DWT

(e) PCNN

(f) NSCT

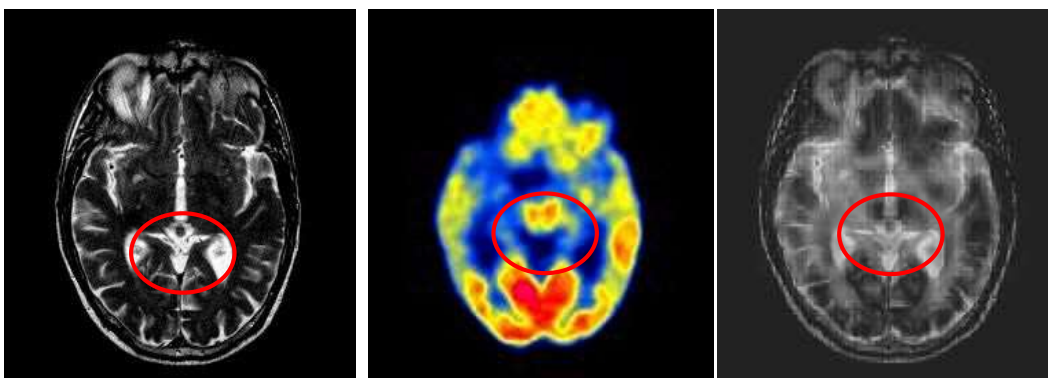


(g) NSST



(h) Proposed Method (NSST-PCNN)

Fig. 9 Experimental results for alzheimer's disease affected images (Set 5)



Hybrid Integration of Transforms with Neural Network based Fusion Techniques for clinical and Healthcare Applications

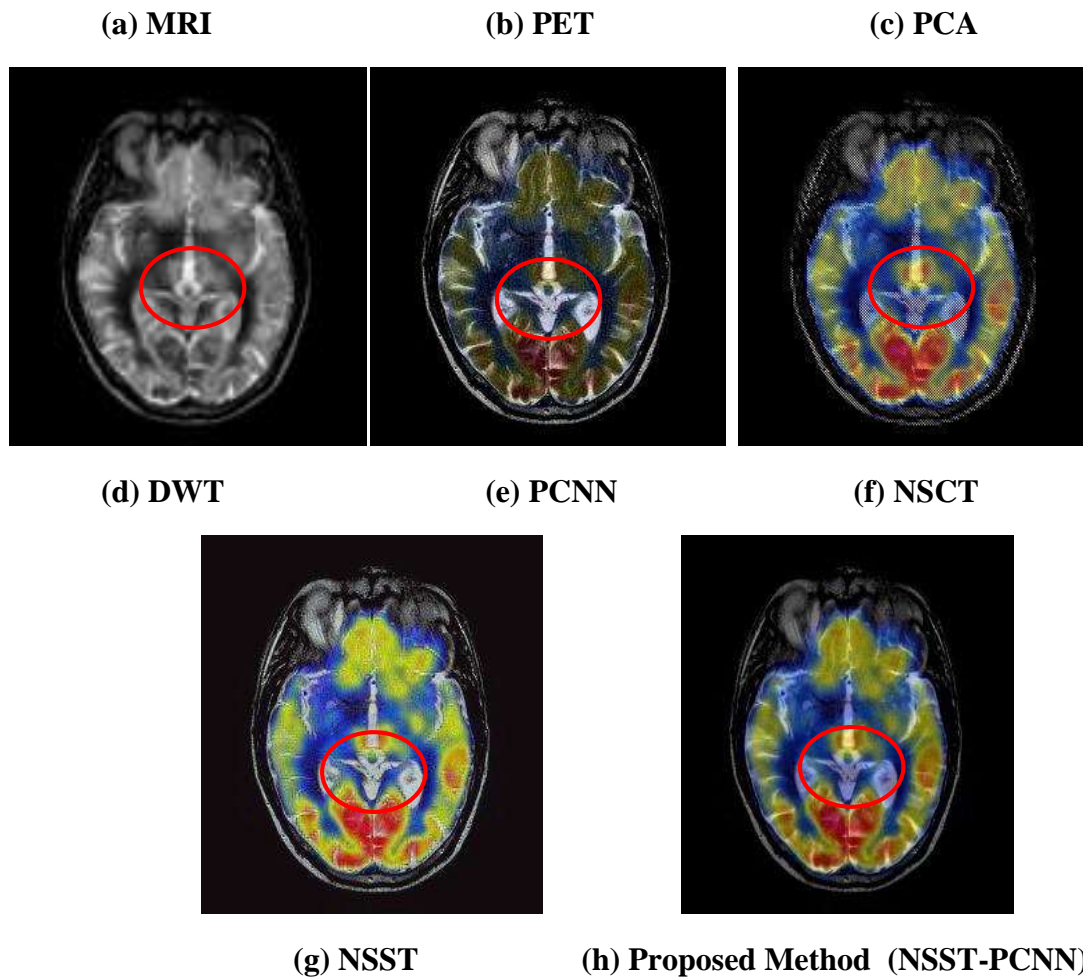


Fig. 10 Experimental results for mild Alzheimer's disease affected images(Set 6)

To improve the efficiency of fusing images, performance metrics values' limits of fusion factor needs to be the highest value, the IQI, mSSIM, EQM and cross entropy must be obtaining the highest value. If the value is more or less '1' then is the fused output image is of improved quality. Comparison is done between the hybrid fusion algorithm and other pre-existing fusion algorithms namely PCA, DWT, NSCT, NSST and PCNN. [21]

Table 1 Performance Metrics Comparative analysis for different fusion methods (Set 1, Set 2 and Set 3)

Study Set	Metrics \ Algorithm	FusFac	IQI	mSSIM	CE _n	EQM	MI	PSNR	STD
	Set 1	PCA	2.187	0.401	0.472	2.261	0.471	2.903	29.60
DWT		2.265	0.522	0.499	2.174	0.522	2.998	32.43	17.20
PCNN		2.471	0.581	0.516	2.017	0.571	2.801	32.53	16.40
NSCT		2.693	0.605	0.542	1.997	0.605	2.703	33.70	23.54
NSST		2.880	0.698	0.681	1.378	0.638	3.205	37.70	25.78
Proposed (NSST-PCNN)		5.012	0.925	0.891	0.782	0.925	3.803	47.60	30.32
Set 2	PCA	1.316	0.498	0.452	1.272	0.719	2.403	30.12	17.39

	DWT	2.362	0.511	0.502	1.182	0.728	2.684	33.50	18.30
	PCNN	2.712	0.532	0.629	1.198	0.767	2.530	32.65	19.50
	NSCT	2.862	0.582	0.635	1.207	0.801	2.839	34.67	25.67
	NSST	3.298	0.682	0.699	1.101	0.837	2.973	39.43	28.67
	Proposed (NSST-PCNN)	4.701	0.891	0.942	0.887	0.942	3.570	48.56	32.54
Set 3	PCA	2.571	0.514	0.523	1.452	0.517	2.402	28.60	18.30
	DWT	2.671	0.538	0.443	1.298	0.529	2.503	29.60	19.30
	PCNN	2.712	0.554	0.585	1.389	0.534	2.603	29.65	23.54
	NSCT	2.811	0.597	0.594	1.078	0.597	2.703	32.60	25.40
	NSST	3.181	0.662	0.702	0.993	0.698	3.012	39.80	26.40
	Proposed (NSST-PCNN)	5.012	0.897	0.891	0.725	0.951	3.602	49.70	31.20

Table 2 Performance Metrics Comparative Analysis for different fusion methods (Set 4, Set 5 and Set 6)

Study Set	Metrics	FusFac	IQI	mSSIM	CE _n	EQM	MI	PSNR	STD
	Algorithm								
Set 4	PCA	2.351	0.498	0.4016	2.012	0.681	2.503	28.67	24.30
	DWT	2.412	0.521	0.528	1.992	0.712	2.865	29.60	25.76
	PCNN	2.561	0.559	0.561	1.862	0.751	2.903	30.45	27.40
	NSCT	2.718	0.571	0.581	1.251	0.781	2.863	32.50	28.64
	NSST	3.181	0.621	0.691	1.162	0.801	3.196	34.60	29.54
	Proposed (NSST-PCNN)	5.178	0.881	0.956	0.974	0.925	3.650	44.50	34.40
Set 5	PCA	2.151	0.498	0.517	1.312	0.519	2.730	28.60	21.54
	DWT	3.322	0.501	0.521	1.251	0.527	2.832	29.50	23.60
	PCNN	3.376	0.529	0.556	1.102	0.551	2.750	31.50	24.64
	NSCT	3.214	0.543	0.581	0.998	0.571	2.849	34.59	26.07
	NSST	3.428	0.681	0.609	0.981	0.651	3.064	36.50	27.60
	Proposed (NSST-PCNN)	4.019	0.951	0.891	0.698	0.971	3.503	43.50	33.56
Set 6	PCA	2.312	0.567	0.534	1.162	0.634	2.201	28.50	20.10
	DWT	2.471	0.618	0.525	1.052	0.625	2.578	29.54	24.03
	PCNN	2.528	0.630	0.542	1.592	0.632	2.720	31.45	23.30
	NSCT	2.692	0.655	0.575	1.224	0.655	2.842	34.65	26.32
	NSST	2.982	0.725	0.698	1.092	0.708	3.206	35.49	28.32
	Proposed (NSST-PCNN)	4.221	0.911	0.941	0.692	0.951	3.703	45.69	34.20

Hybrid Integration of Transforms with Neural Network based Fusion Techniques for clinical and Healthcare Applications

In table 1 and 2 quantitative evaluation, first best results described with block color with bold and the second-best results described with red colors to give a better indication. These methods are employed alongside fusion rules as averaging for approximate subband coefficients as well as highest value chosen for high-pass subband coefficients. Qualitative and quantitative assessment is performed for the presented algorithm. Qualitative analysis is performed by the radiology experts by visual assessment; Estimation of the fusion parameters are done as quantitative analysis. It is clear that the proposed NSST – PCNN method performs better than the conventional methods.

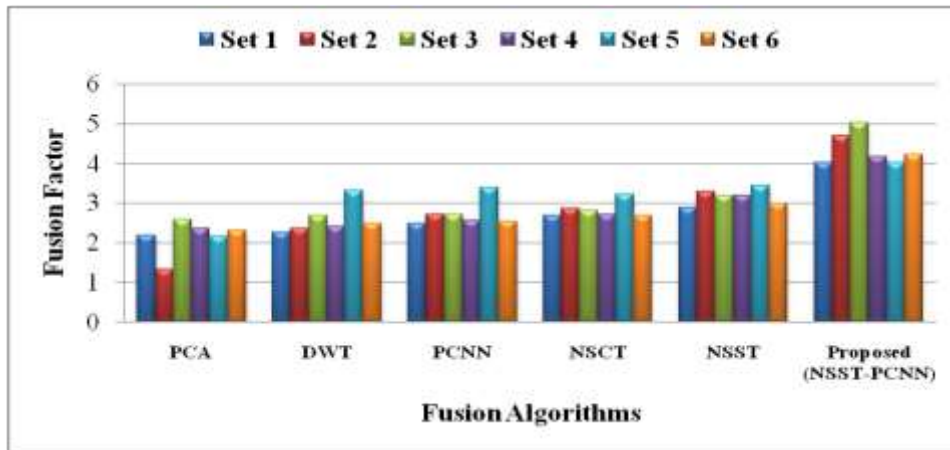


Fig. 11 Comparative Analysis for Fusion Factor

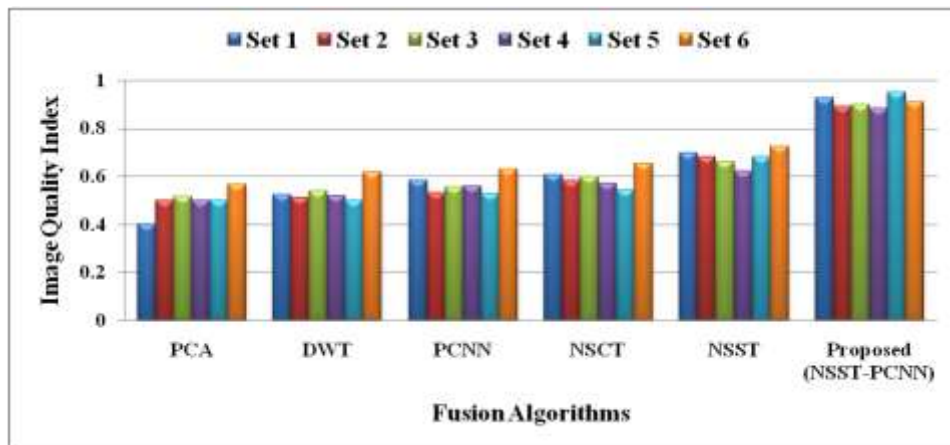


Fig. 12 Comparative Analysis for Image Quality Index

Figures 11 and 12 show the fusion factor and IQI for the six set of images CT-MRI, MRI-SPECT, MRI-PET. The results of experiments are weighed up with PCA, DWT, PCNN, NSCT and NSST methods. The proposed NSST- PCNN has higher fusion factor and IQI value in comparison to the traditional methods.

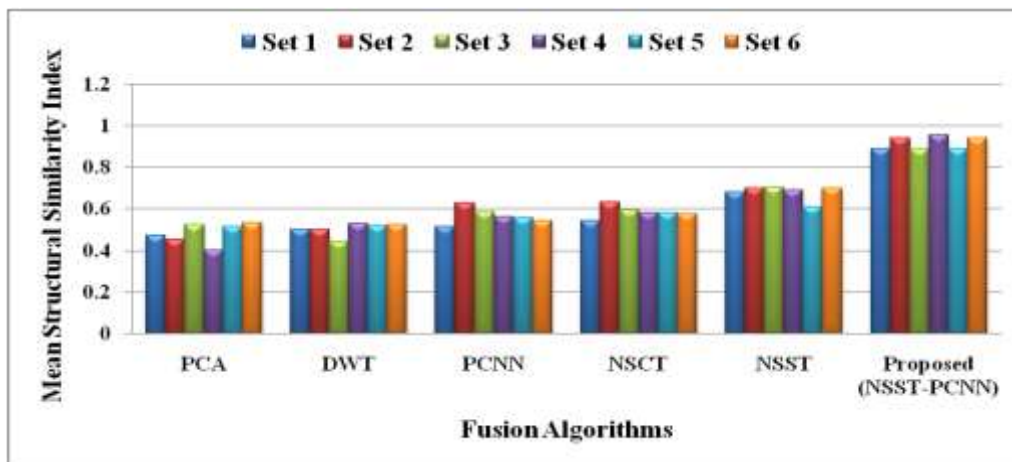


Fig. 13 Comparative Analysis for mean Structural Similarity Index

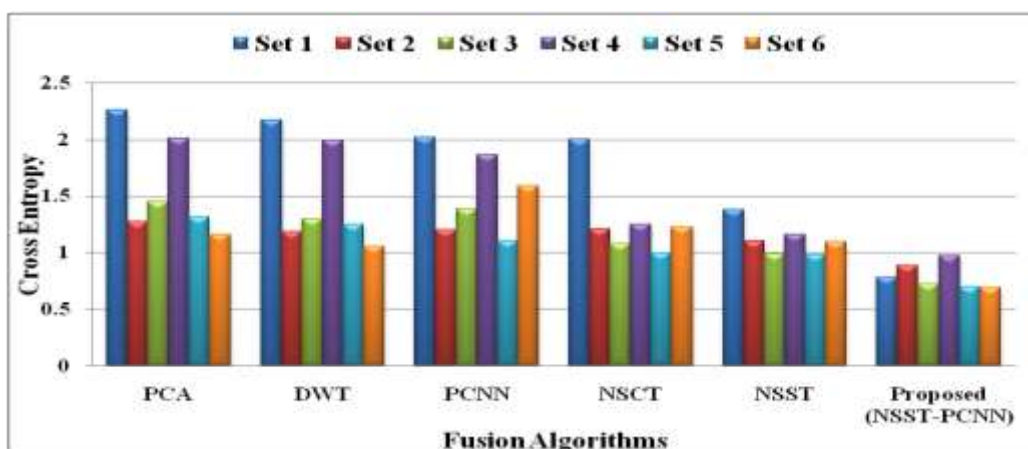


Fig. 14 Comparative Analysis for Cross Entropy

Figures 13 and 14 show the comparative analysis for the mSSIM and cross entropy for the six set of images CT-MRI, MRI-SPECT, MRI-PET. The study results are weighed up with PCA, DWT, PCNN, NSCT and NSST techniques. This NSST-PCNN has higher value for mSSIM and get lower value for cross entropy in comparison to the traditional methods

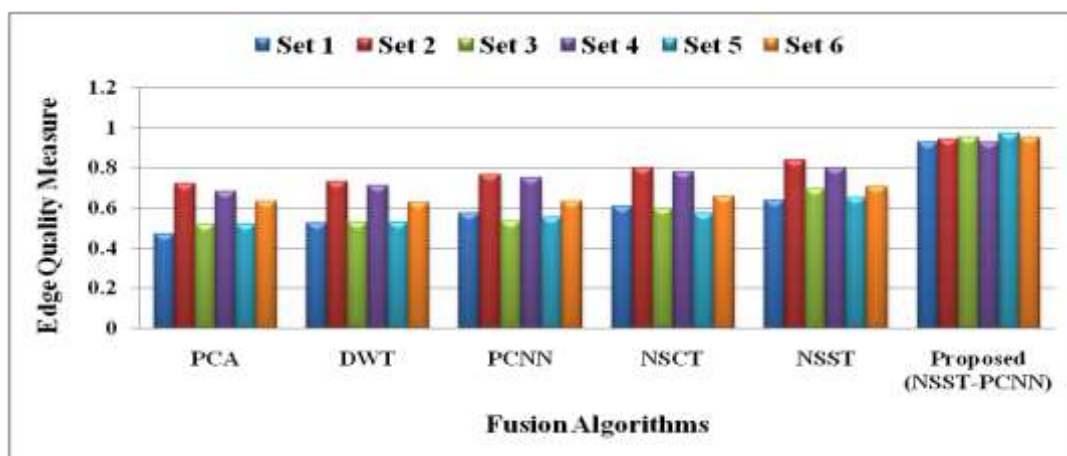


Fig. 15 Comparative Analysis for Edge Quality Measure

Hybrid Integration of Transforms with Neural Network based Fusion Techniques for clinical and Healthcare Applications

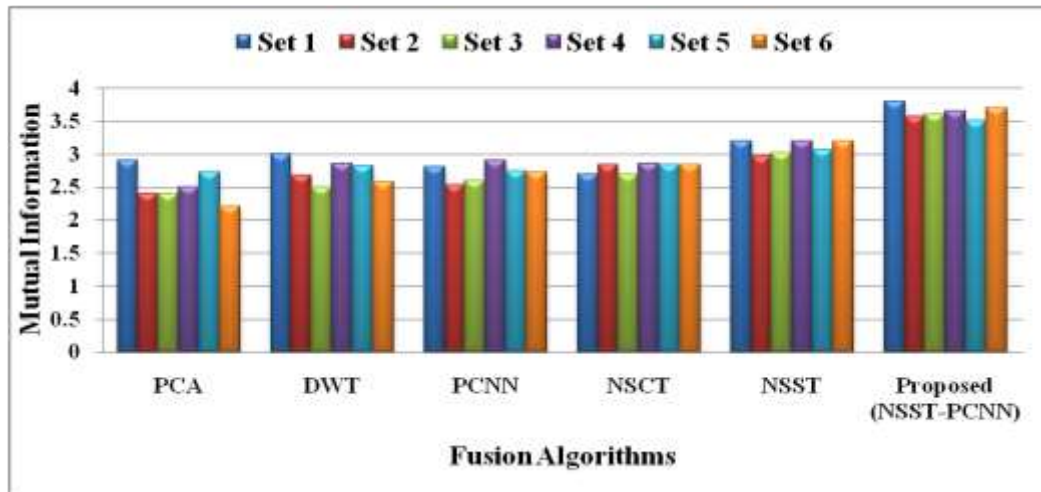


Fig. 16 Comparative Analysis for Mutual Information

Figures 15 and 16 show the comparative analysis for the EQM and MI for the six set of images CT-MRI, MRI-SPECT and MRI-PET. The study results are weighed up with PCA, DWT, PCNN, NSCT and NSST techniques. This NSST-PCNN has higher value for EQM and MI in comparison to the traditional methods

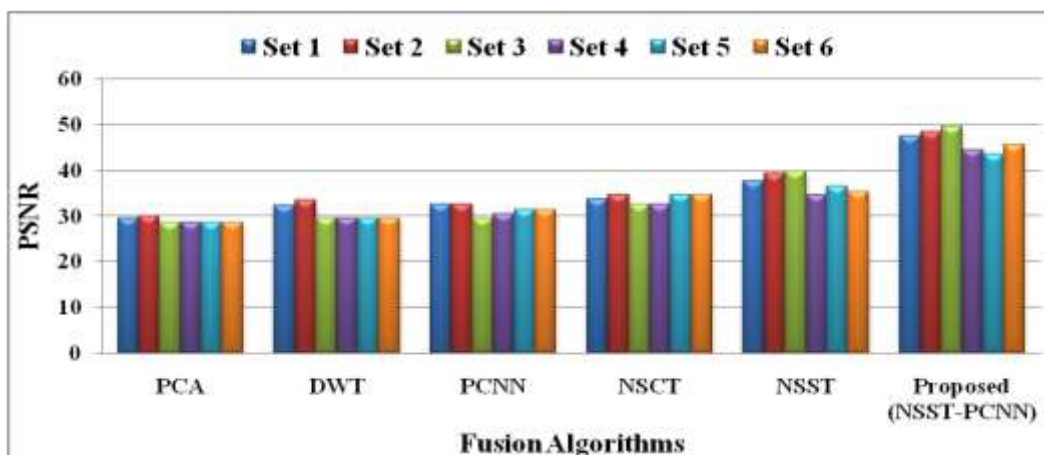


Fig. 17 Comparative Analysis for PSNR

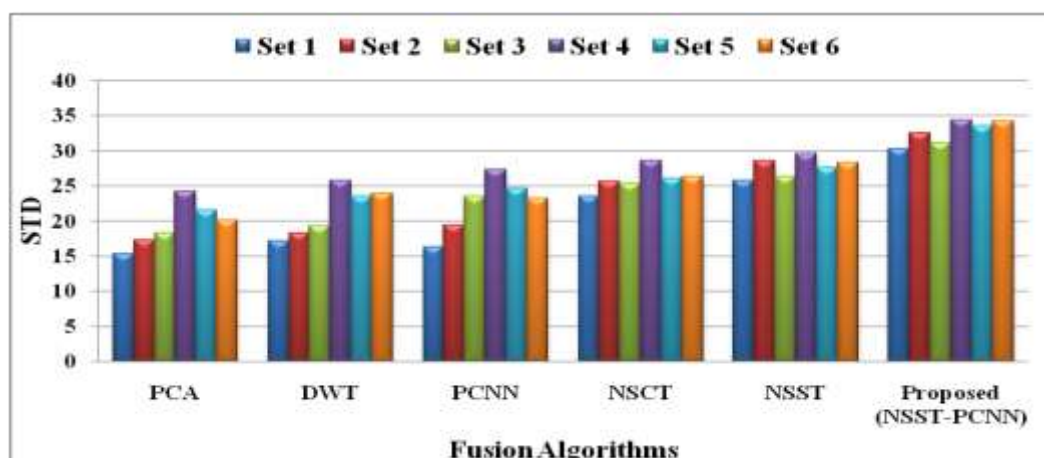


Fig. 18 Comparative Analysis for standard deviation

Figures 17 and 18 show the comparative analysis for the PSNR and standard deviation for six sets of images CT-MRI, MRI-SPECT, MRI-PET. The study results are weighed up with PCA, DWT, PCNN, NSCT and NSST technique. This NSST- PCNN has higher value for PSNR and standard deviation in comparison to the traditional methods

5. CONCLUSIONS

In this paper, multimodal medical image fusion has been performed using NSST with PCNN based hybrid algorithm. Pixel based activity measurement was used. The PCNN uses the modulatory coupling. The average fusion rule is applied for fusing the low frequency region, and the maximum coefficient rule is used for fusing the high frequency region. The results are compared with the conventional PCA, DWT, PCNN, NSCT and NSST method. Objective and subjective evaluation of the fused images was carried out. The performance evaluation shows that this method outperform the traditional methods with respect to information content, the data spread and the volume of information shared from the source images to the fused image. The results are also compared with the recent research work, going on in the field of image fusion. The performance metrics used for the comparisons are fusion factor, IQI, EQM and mSSIM, cross entropy, MI, standard deviation and PSNR. Compared to the existing works, the NSST – PCNN based hybrid method gives good characteristics for the fused image.

REFERENCES

1. Lei Wang Bin Li and Lian-fang Tian, (2014), Multi-modal medical image fusion using the inter-scale and intra-scale dependencies between image shift-invariant shearlet coefficients, *Information Fusion, Elsevier*, Vol.19, pp.20-28.
2. Lei Wang, Bin Li and Lian-fang Tian, (2014), EGGDD: An explicit dependency model for multi-modal medical image fusion in shift-invariant shearlet transform domain, *Information Fusion, Elsevier*, Vol.19, pp.29–37.
3. Jingming Yang, YanyanWu, Yajie Wang and Yulin Xiong, (2016), A Novel Fusion Technique for CT and MRI Medical Image Based on NSST, *IEEE 28th Chinese Control and Decision Conference (CCDC)*, Vol.28, pp.4367–4372.
4. Niu Ling and Duan Mei-Xia, (2016), Fusion for Medical Images based on Shearlet Transform and Compressive Sensing Model, *International Journal of Signal Processing, Image Processing and Pattern Recognition*, Vol.9(4), pp.1-10.
5. Narasimha, K.N., Murthy and Kusuma, J., (2017), Fusion of Medical Image Using STSVD, *Proceedings of the 5th International Conference on Frontiers in Intelligent Computing: Theory and Applications, Springer*, Vol.516(2), pp.69-79.
6. Xingbin Liu, Wenbo Mei and Huiqian Du, (2018), Multi-modality medical image fusion based on image decomposition framework and non-subsampled shearlet transform, *Biomedical Signal Processing and Control, Elsevier*, Vol.40, pp.343–350.
7. Weiguo Wan, Yong Yang and Hyo Jong Lee, (2018), Practical remote sensing image fusion method based on guided filter and improved SML in the NSST domain, *Signal, Image and Video Processing, Springer*, Vol.12(5),pp.959–966.
8. Weiwei Kong and Jing Ma, (2018), Medical Image Fusion Using Non-subsampled Shearlet Transform and Improved PCNN, *Intelligence Science and Big Data Engineering, Springer*, Vol.11266, pp.635–645.
9. Ming Yin, Xiaoning Liu, Yu Liu and Xun Chen, (2018), Medical Image Fusion with Parameter-Adaptive Pulse Coupled-Neural Network in Nonsubsampled Shearlet Transform Domain, *IEEE Transactions on Instrumentation and Measurement*, Vol.68(1), pp.49–64.

10. Lu Tang, Chuangeng Tian and Kai Xu, (2017), IGM-based perceptual multimodal medical image fusion using free energy motivated adaptive PCNN, *International Journal Imaging System Technology*, Wiley, Vol.28(2), pp.1–7.
11. Xin Jin, Gao Chen , Jingyu Hou , Qian Jiang , Dongming Zhou and Shaowen Yao, (2018), Multimodal Sensor Medical Image Fusion Based on Non-sub sampled Shearlet Transform and S-PCNNs in HSV Space, *Signal Processing, Elsevier*, Vol.153, pp.379-395.
12. Jingming Xia, Yiming Chen, Aiyue Chen and Yicai Chen, (2018), Medical Image Fusion Based on Sparse Representation and PCNN in NSCT Domain, *Computational and Mathematical Methods in Medicine, Hindawi*.Vol.2018, pp.1-12.
13. Weiwei Kong and Jing Ma, (2018), Medical Image Fusion Using Non-subsampled Shearlet Transform and Improved PCNN, *Intelligence Science and Big Data Engineering, Springer*, Vol.11266, pp.635–645.
14. Kai-jian Xia, Hong-sheng Yin and Jiang-qiang Wang, (2018), A novel improved deep convolutional neural network model for medical image fusion, *Cluster Computing, Springer*, Vol.22(1), pp.1515-1527.
15. Sharma Dileepkumar Ramlal, Jainy Sachdeva, Chirag Kamal Ahuja and Niranjana Khandelwal, (2018), Multimodal medical image fusion using non-subsampled shearlet transform and pulse coupled neural network incorporated with morphological gradient, *Signal, Image and Video Processing, Springer*, Vol.12(8), pp.1479-1487.
16. B.Rajalingam, R.Priya, R.Bhavani., Hybrid Multimodal Medical Image Fusion Algorithms for Astrocytoma Disease Analysis. *Emerging Technologies in Computer Engineering: Microservices in Big Data Analytics, Springer*, Vol. 985, 2019, pp. 336–348
17. B.Rajalingam, R.Priya, R.Bhavani., Hybrid Multimodal Medical Image Fusion Using Combination of Transform Techniques for Disease Analysis. *Procedia Computer Science, Elsevier*, Vol. 152, 2019, pp. 150-157
18. B.Rajalingam, R.Priya, R.Bhavani., Multimodal Medical Image Fusion Using Hybrid Fusion Techniques for Neoplastic and Alzheimer’s Disease Analysis, *Journal of Computational and Theoretical Nanoscience*, Vol. 16, 2019, pp. 1320–1331
19. Nawaz, H., Maqsood, M., Afzal, S. *et al.* A deep feature-based real-time system for Alzheimer disease stage detection. *Multimed Tools Appl* (2020).
20. Sampaul Thomas, G.A.; Robinson, Y.H.; Julie, E.G.; Shanmuganathan, V.; Nam, Y.; Rho, S. Diabetic Retinopathy Diagnostics from Retinal Images based on Deep Convolutional Networks. Preprints (2020).
21. Aleksei Grigorev, Shaohui Liu, Zhihong Tian, Jianxin Xiong, Seungmin Rho, Jiang Feng, “Delving deeper in drone-based person re-id by employing deep decision forest and attributes fusion” *ACM Transactions on Multimedia Computing, Communications, and Applications*, Vol. 16, No. 1, pp 1–15 (2020).
22. R. Santhoshkumar, M. Kalaiselvi Geetha, J. Arunnehr, ‘SVM-KNN based Emotion Recognition of Human in Video using HOG feature and KLT Tracking Algorithm, *International Journal of Pure and Applied Mathematics*, vol. 117, No. 15, 2017, pp.621-624, ISSN: 1314-3395.
23. R. Santhoshkumar, M. Kalaiselvi Geetha, ‘Deep Learning Approach: Emotion Recognition from Human Body Movements’, *Journal of Mechanics of Continua and Mathematical Sciences (JMCMs)*, Vol.14, No.3, June 2019, pp.182-195, ISSN: 2454-7190.
24. R. Santhoshkumar, M. Kalaiselvi Geetha, ‘Vision based Human Emotion Recognition using HOG-KLT feature’ *Advances in Intelligent System and Computing, Lecture Notes in Networks and Systems*, Vol.121, pp.261-272, ISSN: 2194-5357, Springer https://doi.org/10.1007/978-981-15-3369-3_20

25. R. Santhoshkumar, M. Kalaiselvi Geetha, 'Human Emotion Prediction Using Body Expressive Feature', *Microservices in Big Data Analytics, IETE Springer Series*, ISSN 2524-5740, 2019, (Springer), https://doi.org/10.1007/978-981-15-0128-9_13
26. R. Santhoshkumar, M. Kalaiselvi Geetha, 'Emotion Recognition System for Autism Children Using Non-verbal Communication', *International Journal of Innovative Technology and Exploring Engineering (IJITEE)*, Vol.8, No.8, June 2019, pp.159-165, ISSN: 2278-3075.
27. P.Deepan and L.R. Sudha, "Object Detection in Remote Sensing Aerial Images: A Review", *International Journal of Scientific Research in Computer Science Applications and Management Studies*, Vol. 7, Issue 4, pp.11-18, 2018. ISSN 2319 – 1953, (UGC Approved)
28. P.Deepan and L.R. Sudha, "Fusion of Deep Learning Models for Improving Classification Accuracy of Remote Sensing Images", *Journal of Mechanics of Continua and Mathematical Sciences*, Vol.14, pp.189-201, 2019. ISSN: 2454-7190, (Web of Science)
29. P.Deepan and L.R. Sudha, "Object Classification of Remote Sensing Image Using Deep Convolutional Neural Network", *The Cognitive Approach in Cloud Computing and Internet of Things Technologies for Surveillance Tracking Systems*, pp.107-120, 2020. <https://doi.org/10.1016/B978-0-12-816385-6.00008-8>
30. <https://www.med.harvard.edu/aanlib> (accessed 2017)
31. <https://radiopaedia.org/articles/neurocysticercosis> (accessed 2017)